

Cambridge University Press

978-1-107-40572-1 - Materials Research Society Symposia Proceedings: Volume 51:
Beam-Solid Interactions and Phase Transformations

Editors: H. Kurz, G. L. Olson and J. M. Poate

Excerpt

[More information](#)

PART IA

PLENARY REVIEWS I

**Laser-Solid and
Surface Interactions**

Cambridge University Press

978-1-107-40572-1 - Materials Research Society Symposia Proceedings: Volume 51:
Beam-Solid Interactions and Phase Transformations

Editors: H. Kurz, G. L. Olson and J. M. Poate

Excerpt

[More information](#)

Cambridge University Press

978-1-107-40572-1 - Materials Research Society Symposia Proceedings: Volume 51:
Beam-Solid Interactions and Phase Transformations

Editors: H. Kurz, G. L. Olson and J. M. Poate

Excerpt

[More information](#)

3

PULSED LASER INTERACTIONS WITH CONDENSED MATTER

N. BLOEMBERGEN

Division of Applied Sciences, Harvard University, Cambridge, MA 02138

ABSTRACT

The primary interaction is the absorption of photons by electrons. In metals free-free transitions increase the energy of the electron gas. In semiconductors and insulators electron-hole pairs are created, if the photon energy exceeds the band gap. If it is less, only multiphoton processes can initiate energy transfer from the light beam. In nearly all solid materials Auger processes and electron-phonon interactions occur on a picosecond time scale for the high density and energy of the carrier gas created by intense short laser pulses. Thus melting and evaporation of the material can occur on this time scale. These processes may be considered as the initial phases in the creation of laser produced plasmas. They have been studied by time-resolved measurements of the complex index of refraction, by electron and ion emission, by second harmonic generation, by electrical conductivity and other techniques. Fast time resolution is essential. The dynamic behavior of atoms and phase transitions in the picosecond and femtosecond regime has been opened up for experimental investigation.

1. INTRODUCTION

The basic dissipative interaction process of light with matter is the absorption of light by electrons. In the infrared the light may be absorbed by optical phonons. The electrons in excited states transfer their energy to other electrons and lattice vibrational modes. The infrared excited optical phonons will also share their energy with other phonons. Heating of the material will result. In metals the dominant absorption mechanism is by the excitation of conduction electrons in inelastic free-free transitions. Such transitions in a collisional plasma are sometimes described as inverse bremsstrahlung. At long wavelengths and electron energies at a few eV, the process is also well described by a high frequency conductivity.

In semiconductors and insulators, the dominant absorption process is the creation of an electron-hole pair, if the photon energy exceeds the band gap. For photons below the band gap, carriers may be created by two-photon (or multi-photon) processes. Stepwise excitation through discrete levels in the band gap is also possible. Once the carrier density has become sufficiently high, additional absorption by the same mechanism as in metals will take place.

In transparent insulators, the absorption is so low that usually no significant absorption and heating occurs, until the light intensity is raised to such high values that a plasma is formed by dielectric breakdown. Then further absorption by the carriers in the plasma takes place. The initial electrons are either created by ionization of impurities, by multiphoton absorption or, at extremely high intensities, by tunneling during one half light cycle. At lower intensities nonlinear optical interactions in a transparent dielectric will occur. These are usually of a purely parametric nature and do not give rise to energy dissipation. A hybrid form is presented by the stimulated Raman effect, in which energy is deposited in Raman active phonon modes.

This introductory overview is restricted to strongly absorbing materials, in which the energy is deposited in a relatively thin layer of thickness α^{-1} , where α is the absorption coefficient. The light intensity decays as $I = I_0 \exp(-\alpha z)$ as it penetrates into the medium normal to the boundary at $z = 0$. The results of the interaction depend strongly on the power level and on the pulse duration of the irradiation. The salient features of the interaction

in each regime are reviewed, when surfaces of metals or semiconductors are irradiated at increasing power flux densities with millisecond, microsecond, nanosecond, picosecond and femtosecond duration pulses, respectively.

2. INTERACTION WITH MILLISECOND TO NANOSECOND PULSES

For these relatively long irradiation times a quasi-steady state develops. The absorption depth $d_{\text{abs}} = \alpha^{-1}$ is generally small compared to the heat diffusion length, $d_{\text{diff}} \approx (t_p \kappa)^{1/2}$, during the pulse duration t_p . Here $\kappa = K/\rho C$ is the thermal diffusivity, K is the thermal conductivity, ρ the density, and C the specific heat per unit mass. For metals κ lies in the range of 0.1-1 in cgs units. So, d_{diff} is about 10^{-2} cm for $t_p = 10^{-3}$ s and 10^{-5} cm at $t_p = 10^{-9}$ s. In metals $d_{\text{abs}} \approx (3-5) \times 10^{-6}$ cm, the London penetration depth in a strongly collisional plasma, largely independent of the wavelength for $\omega \tau \ll 1$. For silicon $d_{\text{abs}} \approx 10^{-5}$ cm for green light at room temperature. It is shorter for shorter wavelengths and at higher temperatures. Liquid silicon is metallic.

At low intensities the temperature rise at the surface will be small, and the rise will be determined mostly by convective cooling in the atmosphere. For power flux densities exceeding 1 kW/cm^2 , neither convective cooling nor radiative cooling plays a significant role. For a black body at 3347°K , the radiative flux equals 1 kW/cm^2 , while the convective cooling at a Mach number of one by a flowing gas over a surface at this temperature is less than 100 W/cm^2 . The heat balance is largely determined by heat diffusion into the interior of the material or by evaporative losses. Since the thickness of the sample d is usually more than a few mm, one has $d > d_{\text{diff}}$ and the back face remains essentially at room temperature. A one-dimensional heat balance problem results if the beam diameter is also large compared to d_{diff} . The average temperature rise near the front surface may be estimated by assuming that a volume of depth d_{diff} is heated uniformly

$$(kt_p)^{1/2} \rho C_v (T - T_0) \approx (1-R) I_0 t_p \quad (1)$$

where RI_0 is the reflected intensity. Thus the temperature rise is proportional to the power flux density and the square root of the pulse duration, or proportional to the energy fluence and inversely proportional to the square root of the pulse duration. It is easy to reach the melting point, or indeed the boiling point, of any material with laser flux densities of 10 kW/cm^2 or more. Thus laser welding, drilling, etc., have found widespread applications. Figure 1 is taken from an early standard text [1] to remind the reader what happens in the regime of relatively long irradiation times. Detailed numerical solutions of the heat transport equation can take account of the variation of the material constants with temperature, of the latent heat on melting, etc.

When the temperature is elevated so that significant vaporization occurs, a steady state regime may develop for microsecond pulses where the energy absorbed per unit time per unit area is carried away by the evaporated mass. The surface recedes by ablation at a constant speed v_s given by

$$\rho L_v v_s = (1-R) I_0 \quad (2)$$

Here L_v is the heat of evaporation per unit mass. This behavior is illustrated in Fig. 2, where the surface temperature of an Al alloy target, irradiated by a laser flux of 10^7 W/cm^2 is plotted vs time [2]. The mass flow rate ρv_s for evaporation into vacuum may be crudely estimated by taking the saturated vapor pressure at the surface temperature $p(T_s)$ and assuming the flow normally outward from the surface to be described by a one-sided Maxwell-Boltzmann distribution at temperature T_s . This procedure yields

$$\rho v_s = p(T_s)/(2\pi k T_s/m)^{1/2} \quad (3)$$

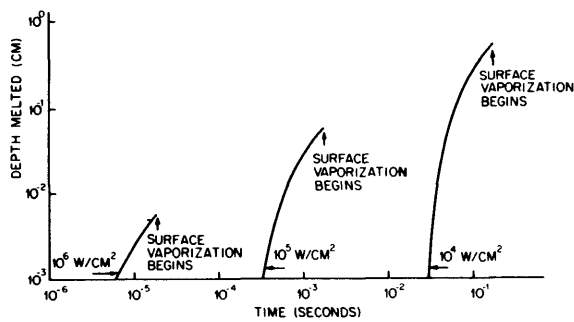


Fig.1. Melted depth in yellow brass as a function of time for various laser flux densities (after ref. 1).

Combination of Eqs. (2) and (3) yields an equation for the steady state surface temperature.

$$\frac{p(T_s)L_v}{(2\pi kT_s/m)^{1/2}} = (1-R) I_0 \tag{4}$$

Since the saturated vapor pressure depends exponentially on the temperature according to the Clausius-Clapeyron equation, the surface temperature will rise only logarithmically with increasing intensity above the boiling point, while the surface ablation rate increases linearly with I_0 .

It may be possible to heat a substance above the critical point, when the intensity is so high that the pressure required to yield the steady state evaporation rate exceeds the pressure at the critical point. In this situation the following model description may be used. The solid material is superheated under pressure to a high temperature. Individual particles are held in a potential well determined by an average bond strength. If the normally directed kinetic energy exceeds the potential well depth, the binding energy per atom in the condensed phase, E_{coh} , the particle will escape. The number of particles escaping per unit area per unit time is given by

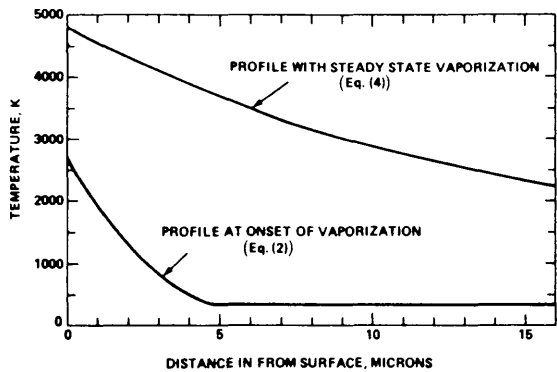


Fig.2. Temperature profiles of an aluminum target absorbing a laser flux $(1-R)I_0 = 10^7 \text{ W/cm}^2$ (after ref. 2).

$$N_0 \frac{1}{(2\pi k T_s m)^{1/2}} \int_0^\infty e^{-\frac{1}{2}(m v_x^2)/(k T_s)} v_x dv_x .$$

$$v_x = \sqrt{\frac{2E_{coh}}{m}}$$

Multiplication by the mass of particle leads to

$$\rho v_s = \rho_s \left(\frac{k T_s}{m} \right)^{1/2} e^{-E_{coh}/k T_s} \tag{5}$$

where ρ_s is the solid density and T_s the surface temperature. This model is, of course, entirely analogous to that of thermionic emission, which describes the evaporation of electrons in the Maxwell-Boltzmann tail of the Fermi-Dirac distribution. In this case E_{coh} is replaced by the work function. It is reassuring that Eq. (3) with the saturation vapor pressure has a similar exponential character as Eq. (5).

It is possible to make these considerations more quantitative. The one-dimensional model of heat diffusion is valid if the laser spot size is large compared to the thickness of the sample and large compared to the thermal diffusion length. The diffusion equation is

$$\rho C \frac{\partial T}{\partial t} = \frac{\partial}{\partial z} \left(K \frac{\partial T}{\partial z} \right) + \alpha (1-R) I_0 \exp - \int_0^z \alpha dz . \tag{6}$$

In this equation the material constants for the density ρ , the specific heat C , the thermal diffusion constant K , the absorption coefficient α and the reflection coefficient R are all functions of the temperature. The boundary condition at the front surface, $z = 0$, is

$$-K \frac{\partial T}{\partial z} + \rho v_s \Delta H_v + \bar{\epsilon} \sigma T^4 + C'(T-T_0) = 0 . \tag{7}$$

Here $\bar{\epsilon}$ is the average emissivity of "grey-body" radiation, $C'(T-T_0)$ represents the heat loss by convection at the front surface, ΔH_v is the enthalpy of vaporization. The occurrence of melting or another phase transition can be incorporated in the model by adding a delta function to the specific heat, $L_m \delta(T-T_m)$, on the left-hand side of Eq. (7), where L_m is the latent heat of melting.

The evaporation process into an atmospheric environment may also be analyzed more precisely by considering a Knudsen-type boundary layer adjacent to the surface. Through this boundary layer the vapor expands into a "rarefaction-wave." This process has been analyzed by Anisimov [3], Krokhin [4] and Knight [5], among others. The result is that the recession rate at a given surface temperature T_s is about 18 percent smaller for a monatomic gas than that given by Eq. (3) or (5). This can be ascribed to gas kinetic collisions in the boundary layer, so that some atoms which have escaped according to those equations are turned back toward the interface.

A more important effect from a practical point of view is that the temperature of the evaporating gas may be so high that a considerable fraction of the evaporating atoms is ionized. If molecules evaporate at high temperature, they may be dissociated. Neutral particles in excited electronic states play an important role in the dynamics of plasma formation by photo-ionization processes. A dense plasma in front of the surface has the consequence that the laser light may now be absorbed by the plasma, rather than by the condensed phase target. These plasma effects have been investigated in great detail both theoretically and experimentally [1,4,6]. They become generally important when the incident power flux density exceeds 10^8 W/cm². Clearly the plasma formation processes will also depend on the presence of an atmosphere in front of the irradiated target.

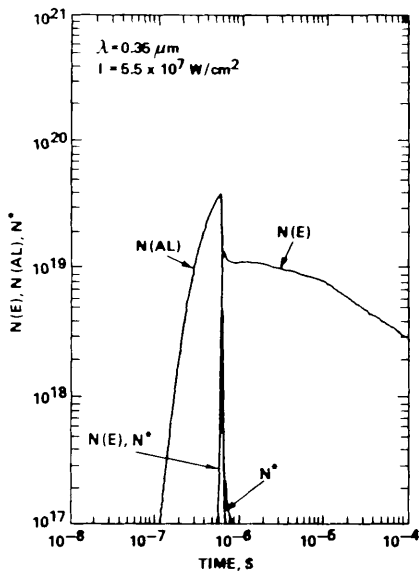


Fig.3. Calculated species densities (Al atoms, excited Al atoms and electrons) vs time for an incident laser intensity of $5.5 \times 10^7 \text{ W/cm}^2$. The reflection coefficient of the alloy at $\lambda = 0.35 \mu\text{m}$ is assumed to be $R = 0.75$ (after ref. 2).

Figure 3 illustrates the initial stages of plasma formation [2] in front of an aluminum alloy in vacuo, which is irradiated by a microsecond pulse from an excimer laser at $\lambda = 0.35 \mu\text{m}$. It may be concluded that the interaction of laser pulses with condensed matter is well understood in the regime where the pulse length is longer than 10^{-9} s and the maximum power flux density is less than 10^8 W/cm^2 .

3. IRRADIATION BY PICOSECOND PULSES

When t_p lies in the range 10^{-12} – 10^{-9} s , we enter the regime where the heat diffusion length becomes comparable to or smaller than the absorption depth $\sqrt{Kt_p} \leq \alpha^{-1}$. When $d_{\text{diff}} \ll d_{\text{abs}}$, the heat is deposited in a layer of constant depth, d_{abs} , and the temperature rise increases linearly with t_p . The average temperature in the surface layer is proportional to the fluence, and Eq. (1) is replaced by

$$C_v(T-T_0)d_{\text{abs}} = (1-R) \int_0^{t_p} I_0 dt. \quad (8)$$

Since all the light energy is absorbed in a thin layer, the melting point or the evaporation temperature of any metallic material can be reached at modest energy fluence. For example, the melting point of tungsten is reached for 0.1 J/cm^2 at $\lambda = 1.06 \mu\text{m}$ in a 30 ps pulse, and the melting point of silicon is reached for 0.2 J/cm^2 at $\lambda = 0.53 \mu\text{m}$ and $t_p \approx 2 \times 10^{-11} \text{ s}$. On melting, silicon becomes metallic, the absorption depth at $\lambda = 0.53 \mu\text{m}$ decreases abruptly from about $2 \times 10^{-5} \text{ cm}$ to $3 \times 10^{-6} \text{ cm}$. It is estimated that at 1 J/cm^2 the silicon surface is heated above the critical point temperature of 5000°K . Significant surface damage due to evaporation may be observed after the irradiation.

It is important to emphasize that practically no evaporation occurs during a picosecond pulse of 10^{-11} s duration, or less. There simply is not enough time for the atoms to move and to establish a steady state evaporation regime.

Consider an elevated surface temperature T_s , where the average thermal velocity in the normal direction is $(kT_s/m)^{1/2}$. The model of evaporation out of a potential well of depth E_{coh} , given by Eq. (5) should describe the situation rather well, as the average time between collisions is longer than t_p , even if the vapor pressure were one thousand atmospheres. The maximum rate of evaporation is $\rho_g(T_s)(kT_s/m)^{1/2}$. During the light pulse the surface of the condensed matter recedes by an amount $d_{evap} = (\rho_g/\rho_s)(kT_s/m)^{1/2}t_p$. Let us take $v_{th} \approx 2 \times 10^5$ cm/s, $t_p \sim 10^{-11}$ s. Even if ρ_g/ρ_s were as large as $\sim 10^{-2}$, which would correspond to a pressure of about six hundred atmospheres for atomic silicon vapor at about 5000°K, one would find $d_{evap} \approx 2 \times 10^{-8}$ cm, or less than one atomic layer of Si would have evaporated during the pulse. Thus the optical thickness of the vapor during the irradiation is negligible. Furthermore, no collisions have taken place and no plasma has developed during the pulse.

Still another way to look at the same situation is as follows. Only atoms at the surface can escape from the condensed phase. These atoms vibrate with a typical Debye frequency, characteristic for phonons at the boundary of the Brillouin zone. This frequency is on the order of 10^{13} s⁻¹. During each vibrational period the atom has a probability for escape equal to $\exp[-E_{coh}/kT_s]$ to overcome the potential barrier. This language is identical to that of a simple Eyring model for molecular dissociation. For $E_{coh} \sim 2.5$ eV and $T_s \sim 0.5$ eV corresponding to 6000°K, the probability for escape on each try is $e^{-5} \approx 0.01$. Again not more than one surface layer will escape during 10^{-11} s.

It is quite likely that a significant fraction of the relatively small number of particles escaping during the pulse is ionized. After the picosecond pulse the surface layer cools very rapidly by heat diffusion into the cold interior substrate. Since the vapor pressure depends exponentially on the temperature, the evaporation rate also diminishes very rapidly on cooling. It may be estimated that the number of particles escaping from the metal after the light pulse is of the same order of magnitude as the number escaping during the light pulse. Thus the picosecond pulse regime of heating of strongly absorbing materials is significantly different from that by pulses of a nanosecond or longer, because of the following two inequalities,

$$(\kappa t_p)^{1/2} < d_{abs}, \text{ and } (\rho_g/\rho_s)(kT_s/m)^{1/2}t_p \ll d_{abs}.$$

In the limit $\rho_g/\rho_s = 1$ the last condition becomes $v_{act}t_p \ll d_{abs}$, where v_{act} is the sound velocity. It is possible to raise the condensed matter in less than 10^{-11} s to temperatures well above the boiling point or critical point. Since $d_{abs} \gg v_{th}t_p$, the atoms have no time to move over significant distance during the pulse, and any absorbing condensed material may be raised to the temperatures in the range of 0.5 – 1×10^4 K and pressures of about 10^3 atmospheres. The incident energy fluence for a 10 ps pulse required to reach this state in materials with an absorption depth $d_{abs} \sim 50$ nm lies typically in the range between 0.3 and 2 J/cm². This corresponds to average power flux densities of about 10^{11} W/cm². Because of the short duration, plasma effects or absorption in the vapor are usually absent.

In laser generation of fusion plasmas with inertial confinement, much higher power flux densities are used, of about 10^{14} W/cm². Then the electric field amplitude is comparable to the Coulomb field, which is responsible for the binding of the valence electrons. During one light cycle considerable numbers of electrons can tunnel out of their orbits. Any material, including transparent dielectrics, is converted into plasma at the solid density during the early stages of the pulse. Thus a dense plasma with initial electron temperature of 10^4 – 10^3 eV is assumed as the initial state. This plasma gets further heated by the bulk of the laser pulse [6].

The present paper focuses on the "pre-plasma" conditions, which are realized for pulses with between 10^{-12} and 10^{-10} s duration and peak power levels below 10^{10} – 10^{11} W/cm². Then the material is characterized by electron temperatures on the order of a few eV or less, and the phonon temperature lies in the range 10^3 – 10^4 K.

In metallic materials the electron-phonon as well as the phonon-phonon interaction times under these conditions are generally shorter than 1 ps, so that local thermodynamic equilibrium prevails in the absence of phase transitions. The very rapid heating rates during the pulse, and the very rapid cooling rates after the pulse, which may amount to 10^{14} K/s, may produce considerable superheating of the solid phase and undercooling of the liquid phase. Phase front boundaries may be driven to velocities of 10^4 cm/sec and molten material may resolidify in amorphous phases. Alloys may retain a composition characteristic of the liquid phase, as there is no time for chemical segregation.

4. PICOSECOND IRRADIATION OF SEMICONDUCTORS

The proceedings of the MRS symposia on laser-beam interactions from 1978 onward provide a detailed history of this topic [7-14]. In a similar general introductory lecture seven years ago, I described the phenomenon of heating on a picosecond time scale [15]. After considerable controversy and discussion, a general consensus has developed that the hot carriers and the lattice in silicon reach a common temperature on a picosecond time scale, and that a silicon surface layer may melt on this same time scale. A threshold value for the fluence inducing melting at the surface of 0.2 J/cm^2 was established for 10^{-11} s pulses at $\lambda = 0.53 \text{ }\mu\text{m}$. Since molten silicon is metallic, an abrupt change in the reflectivity occurs, as shown in Fig. 4. The most detailed information about the nature of the hot layer during and following the pump pulse is obtained by an independent optical picosecond probe pulse [16]. The complex index of refraction is measured by reflection and transmission of a small area in the center of the heated area. Data have been obtained over a wide parameter space, including variation of the pump pulse fluence, time delay between pump and probe, and variation of the probe wavelength from the far-infrared to the near ultraviolet. At long wavelengths the index is predominantly determined by the density of the carrier plasma; at shorter wavelengths the index is determined by indirect band transitions involving the lattice temperature. An illustrative example of the pertinent experimental data on the surface reflectivity as a function of pump fluence 15 ps after the pump pulse at three wavelengths is shown in Fig. 4. With similar data at other delay times, and with data on transmission, the temporal dependence of the

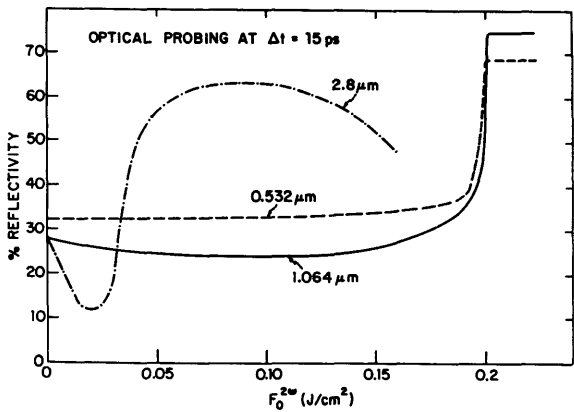


Fig.4. The reflectivity of a silicon crystalline surface at three different wavelengths, 15 ps after a green pump pulse, as a function of pump fluence.

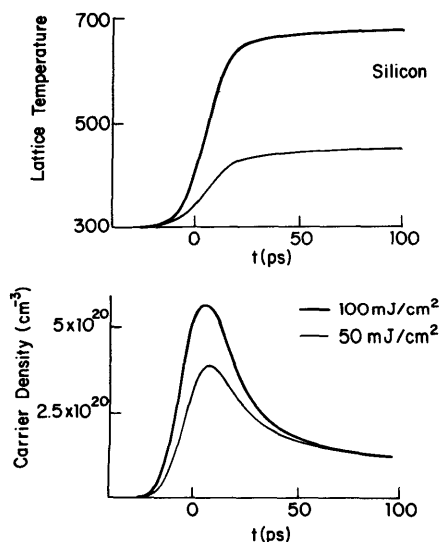


Fig.5. The carrier density and the lattice temperature of a crystalline silicon surface irradiated at $t=0$ by a green pump pulse of 20 ps duration for fluences of 0.05 and 0.1 J/cm², respectively.

carrier density and lattice temperature in crystalline silicon is obtained, as shown in Fig. 5, for two fluences below the melting threshold. The carrier density is limited during and after the pump pulse by Auger recombination. Just before melting, a maximum carrier density of about 1.2×10^{21} /cm³ is obtainable with green pulses of 10^{-11} s duration just before melting sets in. This density is insufficient to induce a transition to another hypothetical solid phase. The lattice temperature falls off slowly, because a rather thick layer of 10^{-5} cm is heated by green light in crystalline silicon.

In the metallic liquid phase the absorption depth is reduced by an order of magnitude. The temperature rises rapidly to the boiling point and beyond the critical point as the fluence is increased to over 1 J/cm². Emission of positive ions and electrons is observed. The velocity distribution of the emitted neutral particles has been measured and is in agreement with a thermal Maxwell-Boltzmann distribution [17]. The velocity distribution of positive ions has also been measured [18]. The average kinetic energy increases with increasing fluence corresponding to a surface temperature of 5000°K, beyond which space charge and dense plasma effects become important. Here one enters a regime characteristic of the picosecond time domain where emission of neutral particles, electrons and positive ions proceeds at comparable rates. The process of the plasma formation is distinct from that discussed earlier, in the microsecond regime.

There are numerous other experimental methods which support the picture of melting and subsequent resolidification. In certain ranges of pump fluence and wavelength, the resolidification occurs so rapidly with such large undercooling of the liquid phase that amorphous silicon may be formed [19,20], as was reported in early 1979. The velocity of the liquid-solid interface has been measured by dc conductivity experiments with nanosecond time resolution. X-ray diffraction has also been accomplished on this time scale, confirming thermal expansion and melting. The post-pulse examination of the surface structure by LEED, Rutherford back scattering and the change in impurity distribution are also powerful tools [7-14]. It may be difficult to improve the temporal resolution of most of these techniques to the picosecond domain. Picosecond electron pulses can, however, be obtained by picosecond photoelectric emission, and picosecond electron diffraction from surfaces has been accomplished [21].